Int. J. Electrochem. Sci., 12 **(2017)** 6010 – 6021, doi: 10.20964/2017.07.58

International Journal of
ELECTROCHEMICAL
SCIENCE
www.electrochemsci.org

Short Communication

Characterization of Copper Coating Electrodeposited on Stainless Steel Substrate

Nik Norziehana Che Isa, Yusairie Mohd[*]*, Mohammad Hafizudden Mohd Zaki and Sharifah Aminah Syed Mohamad*

Faculty of Applied Sciences, Universiti Teknologi MARA,
40450 Shah Alam, Selangor, Malaysia.
[*]E-mail: yusairie@salam.uitm.edu.my

Received: 30 September 2016 / *Accepted:* 11 April 2017 / *Published:* 12 June 2017

The production of copper based products is increased significantly over the years due to a huge industrial interest. This has caused severe depletion of the primary copper ore reserves and the price of solid copper is set to rise. One way of reducing the cost of using solid copper is by producing copper coating which is coated on other cheaper substrates such as stainless steel or aluminum. In this study, copper coating was successfully coated on stainless steel substrate from acidic copper sulfate solution by electrodeposition technique. The characteristic of electrochemical reaction of copper on stainless steel was investigated using cyclic voltammetry. Chronoamperometry was used to further elucidate the nucleation and growth of the copper on stainless substrate. The copper coating was characterized for its surface morphology and crystallography by FESEM and XRD, respectively. A uniform and well adhered copper coating consisting of spherical particles was formed on the stainless steel surface. The particle size, density and surface coverage of copper coating are strongly dependent on deposition conditions (i.e.: applied potential and deposition time) used. XRD patterns confirmed that uniform red-brown color coating deposited on the stainless steel substrate was pure copper with face centered cubic (FCC) crystal lattice. The copper coating can be further investigated for its application for antimicrobial coating.

Keywords: Copper; Copper coating; Cyclic voltammetry; Electrodeposition; Nucleation

1. INTRODUCTION

Copper is considered a semi-precious, nonferrous, malleable metal with many hundreds of applications in a wide range of consumer and industrial applications. The demand of the production of copper is increased significantly over the years due to the rapid growth in the sectors like electricity and electronics, plumbing, construction, architecture, transportation, lifestyle, consumer and health

products [1]. This has caused a harsh reduction of the primary copper ore reserves and the price of raw copper is set to rise. This has led the focus of many researchers to develop new alternative materials to overcome the issues mentioned. Coating copper on fixtures is an attractive and economical alternative to using the solid copper [2-7]. In literatures, various techniques have been used in preparing copper coating and one of them is electrodeposition. Electrodeposition of copper and its alloys has been investigated during the past decades in relation to its particular properties and various applications such as contacts and circuitry in the electronic industry, manufacturing printed-circuit boards, undercoating for other metal thin film coating and the protection and decoration of consumer goods [8-10]. For example, Dini and Snyder [8] have discussed about electrodeposition of copper whilst Walsh and Low [11] have reviewed and highlighted about the electrodeposition of copper alloy (bronze) and its applications which mainly prepared from aqueous electrolytes.

Electrodeposition technique induces relatively lower temperature operation which allowing deposition of copper coating on various substrate surfaces [12]. In addition, it also has ability to coat uniformly on geometrically complex surfaces and to control the thickness and microstructure of the coatings [13]. Electrodeposition of copper has been studied either on copper substrate [14,15] or numerous other substrates including gold [16], platinum [13,14], glassy carbon [13,17], graphite [18,19], aluminum [3-6], stainless steel [20-23] and steel [24,25] from various bath solution formulations [14-16,18,26,27]. Recently, much attention focus on electrodeposition of copper on touch surface metals like aluminum and stainless steel for antimicrobial purposes. Augustin et al. [5] have reported about the effect of current density during electrodeposition of copper on aluminum substrate in terms of microstructure and hardness of textured copper coating and also wettability [6] for antimicrobial touch surface application. In this study, stainless steel substrate was chosen since it is widely used as touch surfaces in the healthcare environment; however, it is no antimicrobial active [16-20].

Copper coating on stainless steel will make the cost down compared to using the solid copper, but adhesive strength between the coating and the substrate is a very critical problem to be tackled. The coating is susceptible to wear and any surface damage which may not only remove the active copper coating, but may introduce scratches which can harbor germs. The improvement in scratch resistance and surface hardness could be achieved by resorting to the formation of nanocrystals in the coating [5]. And, copper films electrodeposited on the metal substrate, usually produced in good adhesive strength if there is no disruption from hydrogen evolution reaction since the films are metallically bound with the substrate [33,34].

A thorough understanding of the relationship between the process parameters, the microstructure and the properties of electrodeposited coating is required in order to tailor its properties and thereby to design the performance [17,35]. Furthermore, a successful development of copper coatings requires the understanding of characteristic and the nature of electrode reactions, nucleation and growth mechanisms. By effectively adjusting the deposition parameters involved, the nature of growth and patterns of the copper coating can be controlled. Although the electrodeposition of copper on stainless steel has been examined [20-22], a number of differences are noted when compared. Since the preparation of copper coating in this study purposely for touch surface applications, certain properties need further attention during the preparation of the copper coating. It is important to

produce smooth and uniform nano-sized crystals of copper coating with good adhesion strength to the substrate for the antimicrobial touch surface application, specifically.

In this paper, the electrodeposition of copper coatings on the stainless steel substrate using of cyclic voltammetry (CV) and chronoamperometry (CA) were discussed. Then, the prepared coatings were characterized for surface morphology and crystallography by FESEM and XRD, respectively.

2. EXPERIMENTAL

2.1 Substrate pre-treatment.

Prior to electrodeposition process, stainless steel substrate, type SS 304 (2 x 2 cm^2) was mechanically polished using SiC papers from P800 to P4000 grit, followed by ultrasonically cleaned with acetone and rinsed with ultra-pure for 15 min each before dried at room temperature. An adhesive tape was used to mask off the stainless steel substrates except surface area of 2 cm^2 in which deposition was desired.

2.2 Electrochemical studies.

The electrochemical studies of copper coated stainless steel were done by cyclic voltammetry (CV) and chronoamperometry (CA). Experiments were carried out in a glass cell with three electrodes: polished stainless steel substrate as working electrode, platinum rod as a counter electrode and Ag/AgCl as a reference electrode, in 0.01 M $CuSO_4$ solution. The solution was prepared using reagent grade of $CuSO_4$ and adjusted to pH 1 by adding concentrated H_2SO_4. CV experiment was carried out by scanning the potential from +0.5 V to -0.5 V and switched back to +0.5 V at a scan rate of 10 mV/s. While, in CA study, the effect of applied potential and deposition time was investigated. Four different potentials (e.g. -0.25 V, -0.3 V, -0.4 V and -0.5 V vs Ag/AgCl) were chosen based on CV result. Whilst, for the effect of deposition time, the electrodeposition of copper on stainless steel at -0.25 V for 60 s up to 900 s, were studied and compared. All experiments were controlled using an Autolab Potentiostat (Aut302 FRA2), interface with a PC running NOVA software and were performed under room temperature.

2.3 Coatings characterization.

Characterization of the prepared copper coatings was obtained by several methods: the surface morphology of the prepared samples was examined by Field Emission Scanning Electron microscope (FESEM, Carl Zeiss SMT Supra 40 VP) and the crystallography and phase structure of the prepared samples were analyzed by a diffractometer (X'pert pro-MPD, PANalytical) with thin film X-ray diffraction (TF-XRD) capability with Cu Kα radiation. The produced patterns were matched with reference pattern available in the X'pert Highscore Plus software.

3. RESULTS AND DISCUSSION

3.1 Stainless Steel Surface Pre-treatment

Surface pre-treatment of the substrates is the critical step before electrodeposition process in order to remove contaminants and oxide layer from the substrate surface. Contaminants and oxide layer will affect the bonding between coating and substrate resulting in poor adhesion. Fig. 1 shows SEM morphologies of the as-received and polished stainless steel surface. The as-received stainless steel seems too rough with imperfections.

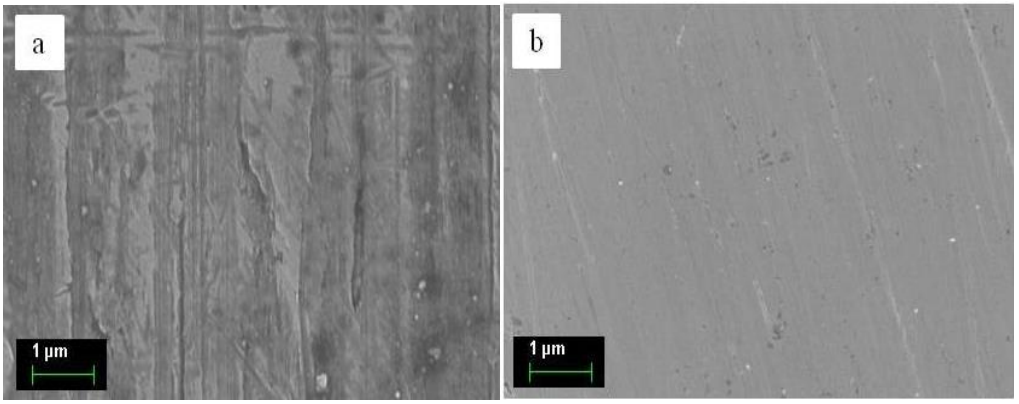

Figure 1. SEM images of the stainless steel surface (a) as-received and (b) after surface pre-treatment process. Magnification: 5000x

After polishing process, the stainless steel surface became more smooth and free from the larger imperfections since small amounts of metal removed by means of abrasives. The removal of the contaminants and oxide layer will make the deposition process possible and improve the adhesion of the coating to the substrate. EDAX analysis was carried out in order to identify the presence of elements on the stainless steel substrate. Table 1 shows the weight percent of the elements present as compared with the standard composition of the stainless steel SS304. It can be seen that the weight percent obtained from EDAX is very close to the standard SS304, confirming that the as-received stainless steel is SS304 type.

Table 1. Elemental compositions of the as-received stainless steel substrate analyzed by EDAX compared to standard SS304

	Weight %	
Element	**From EDAX**	**Standard SS304**
Fe	67.18	65.45
Cr	23.07	18 – 20
C	0.85	0.8
Mn	0.00	Max 2
Ni	8.19	8 – 10.5
P	0.00	Max 0.045
S	0.00	Max 0.03
Si	0.70	Max 1

3.2 Cyclic voltammetry analysis

Fig. 2 shows a cyclic voltammogram of the stainless steel electrode in 0.01 M $CuSO_4$ solution at pH 1 that was scanned from +0.5 V to -0.5 V and switched back to +0.5 V. Analysis of current density versus potential plot is useful to understand the redox reactions involved in the process. From the cyclic voltammogram, it can be described that at the beginning, there was no current observed, meaning that no reaction occurred on the stainless steel electrode surface. Cathodic current starts to increase at a potential of -0.2 V indicated the nucleation of copper on the stainless steel surface. The current density increased continuously until a maximum current at -0.3 V. From -0.2 V to -0.25V, the cathodic process was controlled by electron transfer, while from -0.28 V to -0.32 V, the process was controlled by mixed kinetic process of electron transfer and mass transport. At this potential range, cathodic peak (E_{pc}) was appeared, which corresponds to maximum copper reduction, according to reaction (1).

$$Cu^{2+} + 2e^- \rightarrow Cu \quad (1)$$

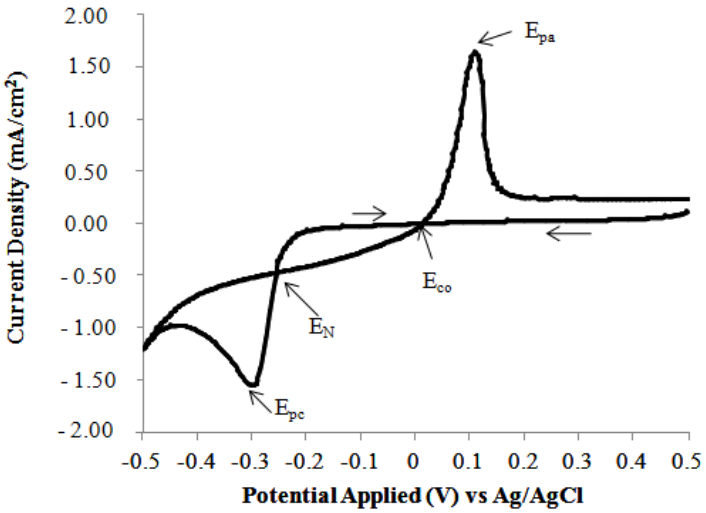

Figure 2. Cyclic voltammogram of stainless steel substrate in solution containing 0.01 M $CuSO_4$ (pH 1) at 25 ^oC. Scan rate: 10 mV/s

After -0.32 V, the current density decreases which the process is controlled by mass transport or diffusion of Cu^{2+}. The decrease of current density may be associated with a depletion of copper species at the interface of the stainless steel electrode surface and indicates there is a nucleation and growth mechanism controlled by diffusion. At more negative potential than -0.48 V, the increase of current is attributed to hydrogen evolution reaction (HER), reaction (2), concurrent with the reduction of copper.

$$2H^+ + 2e^- \rightarrow H_2 \quad (2)$$

Upon sweep reversal (positive scan direction), two crossovers (E_N and E_{co}) were formed. The E_N potential (E = -0.25 V) is a crossover potential at which nucleation and growth take place with a measurable rate known as the nucleation overpotential, which can be employed to estimate the experimental value of nucleation overpotential [26]. While the E_{co} potential (E = +0.02 V) is defined as the crossover potential at which copper starts to undergo either reduction (being deposited) or oxidation (dissolved). The difference in potential between the E_N and E_{co} was due to the nucleation overpotential on stainless steel substrate resulting from the crystallographic misfit between copper and stainless steel [17].

A discussion related to the "crystallographic misfit" statement can be found in literature [17,36]. Deposition potential of metallic ions on a foreign substrate is usually higher than deposition potential on the electrode made of the same metal due to the crystallographic substrate-metal misfit [17]. Therefore, deposition of copper on stainless steel substrate starts at potentials that are more negative than the redox potential of Cu^{2+}/Cu. In the anodic direction, however, the oxidation of copper starts from the stainless steel surface that already has a deposited copper layer, resulting in a potential close to the Cu^{2+}/Cu equilibrium potential. Due to the difference in deposition and dissolution potentials, a crossover occurs between the cathodic and anodic current traces [17,36]. These behaviors are similar with cyclic voltammogram of the nickel electrode in an alkaline copper solution containing glycine reported by Ballesteros et al. [26]. Hence, the presence of the crossover is an indicator for the copper nuclei formation on the stainless steel. At potentials more positive than E_{co}, anodic current increases till the formation of anodic peak (E_{pa}) at E = +0.11 V which corresponds to the reaction (1) in the reverse direction. After peak E_{pa}, current drops to very low current, demonstrating that the dissolution of metallic copper from the stainless steel surface is almost complete.

3.3 Chronoamperometry study

In Chronoamperometry (CA) experiments, two deposition parameters (applied potential and deposition time) were adjusted to investigate the formation of copper coatings. In order to study the effect of applied potential on the formation of the copper nuclei on the stainless steel surface, different potentials were chosen based on CV analysis. The applied potential was set at E_N crossover (-0.25 V) until the lower vertex potential -0.5 V. Fig. 3 shows the chronoamperometric curves of the deposition of copper for 60 s on the stainless steel substrate at different applied potentials. It was found that the current density transient trends were similar with a slight difference in current density values. By increasing the applied potential, the current density became higher. The voltage-current relationship follows Ohm's law concept, with negligible the value of resistance.

The first 5 s was ignored since it indicates the charging of the double layer. Initially, the current density decreased gradually in terms of cathodic current which corresponds to the formation of the first nuclei on the stainless steel electrode. This is followed by a stable current obtained after 40 s due to a further nucleation and growth of copper copper on the stainless steel.

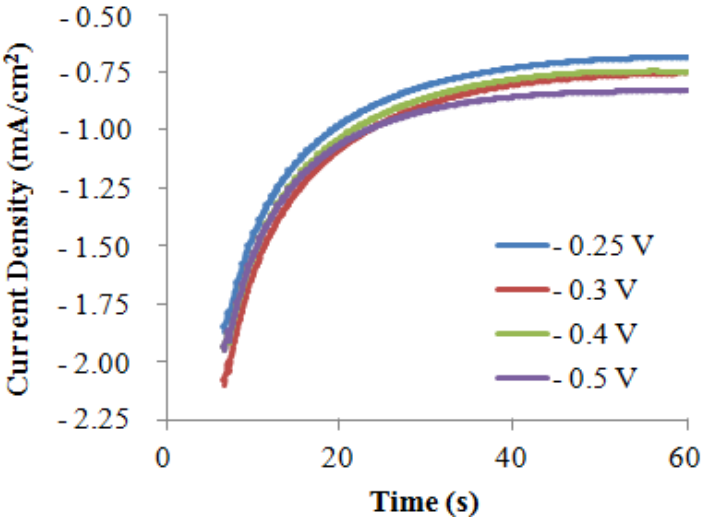

Figure 3. Chronoamperometric curves of the copper coatings on the stainless steel substrate at different deposition potentials

The effect of deposition time on the electrodeposition of copper coatings on the stainless steel substrate was also investigated. The current density as a function of deposition time at -0.25 V was measured and recorded. Fig. 4 shows the chronoamperometric curves of the copper coatings formed on the stainless steel substrate at different deposition times. A similar trend was observed for all curves, except slight difference in terms of current produced which might because of imperfection of the substrate's surface. Plateau current was formed when long deposition time (i.e.: t > 60 s) was applied indicating further development of the copper nucleus on the stainless steel surface. It was found that the copper deposited on the stainless steel substrate in unit time increases with deposition time.

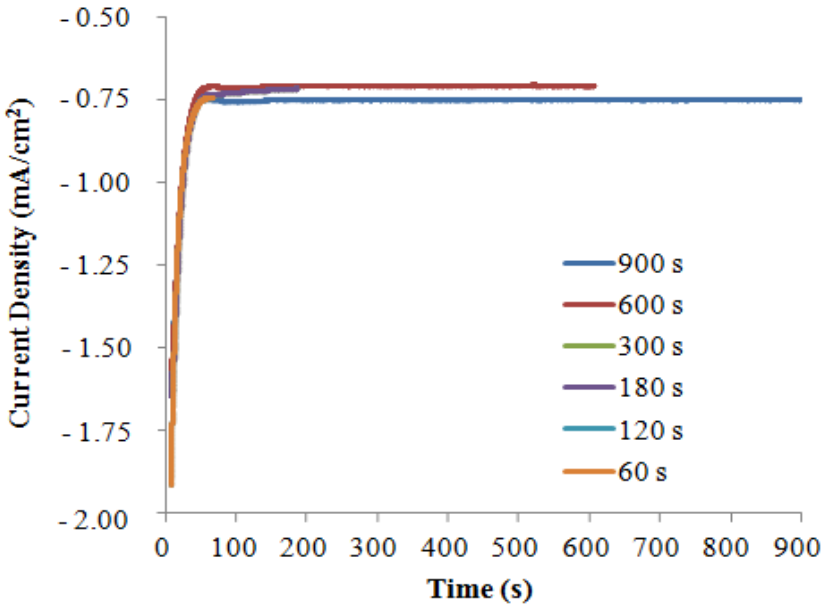

Figure 4. Chronoamperometric curves of the copper coatings on the stainless steel substrate at different deposition times

3.4 Characterization of the copper coatings

The effect of applied potential and deposition time on the electrodeposition process of copper coating on the stainless steel substrate was further characterized. Fig. 5 shows surface morphologies of the copper coatings electrodeposited on the stainless steel surface at different applied potentials. It was found that small copper particles are dispersed on the stainless steel surface with spherical like structures while certain areas of the stainless steel substrate's surface remained bare, for all electrodeposition conditions. However, when increases the applied potential, the amount of copper particles also increased.

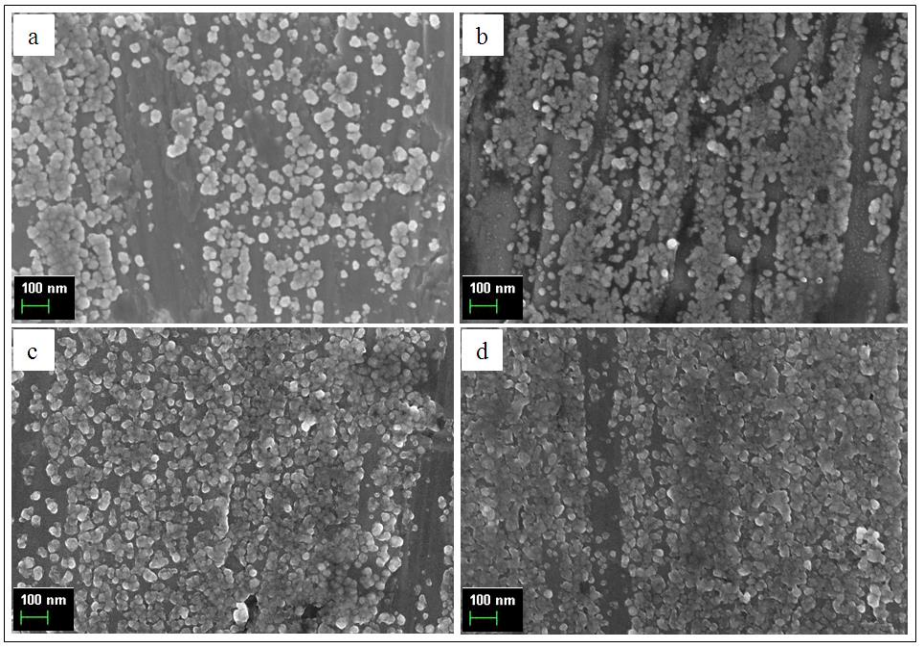

Figure 5. SEM images of the copper coatings on the stainless steel substrate at (a) -0.25 V (b) -0.3 V, (c) -0.4 V and (d) -0.5 V for 900 s

Fig. 6 shows the surface morphologies of the copper coatings electrodeposited at different deposition times at constant applied potential, -0.25 V. At this initial stage, copper more likely to deposit on the defects and voids of the stainless steel surface. After 120s (Fig. 6b), the copper particles cover almost the entire surface of stainless steel. Subsequently, once all of the stainless steel surface covered with copper particles, further increase in deposition time would only increase the size of old particles, obviously seen after 600s of deposition (Fig. 6e). Lengthen the deposition time makes continuation deposition of copper on the stainless steel surface and further development of new copper on the old deposited copper layer.

It is noteworthy to mention that the porous-free structure with nano-sized grain can be formed on the stainless steel surface only after 900 s of deposition (Fig. 6f), since the deposition was done at low deposition applied potential, i.e.: -0.25 V and no incorporation of hydrogen evolution during the electrodeposition process. An even distribution of copper particles with very uniform in size appeared on the stainless steel surface indicating that the electrodeposition mechanism is instantaneous reaction.

Similar observation was obtained by Wang et al. [9] however using copper sulfate-ethylenediamine bath solution at pH 7.45.

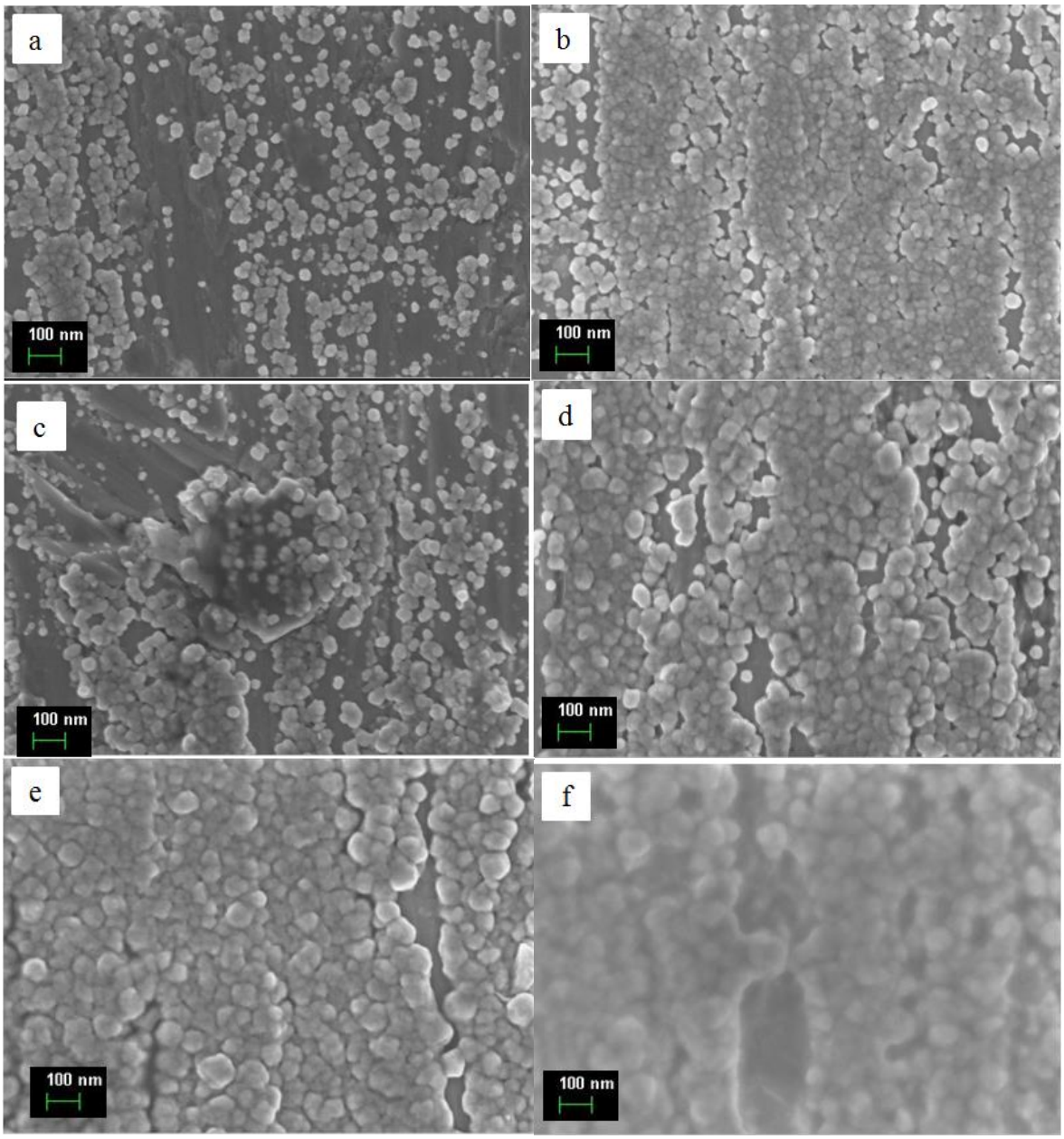

Figure 6. SEM images of the copper coatings on the stainless steel substrate at -0.25 V for (a) 60 s, (b) 120 s, (c) 180 s, (d) 300 s, (e) 600 s and (f) 900 s

Fig. 7 shows visual observation of copper coatings electrodeposited on the stainless steel surface at different deposition times. It can be seen obviously that the entire stainless steel surface exposed (i.e.: 2 cm^2 in bath solution during electrodeposition process) was covered with smooth and uniform coatings with red-brown color. Lengthen the deposition time allows more copper deposited on the stainless steel surface and resulted in a darker red-brown color coating.

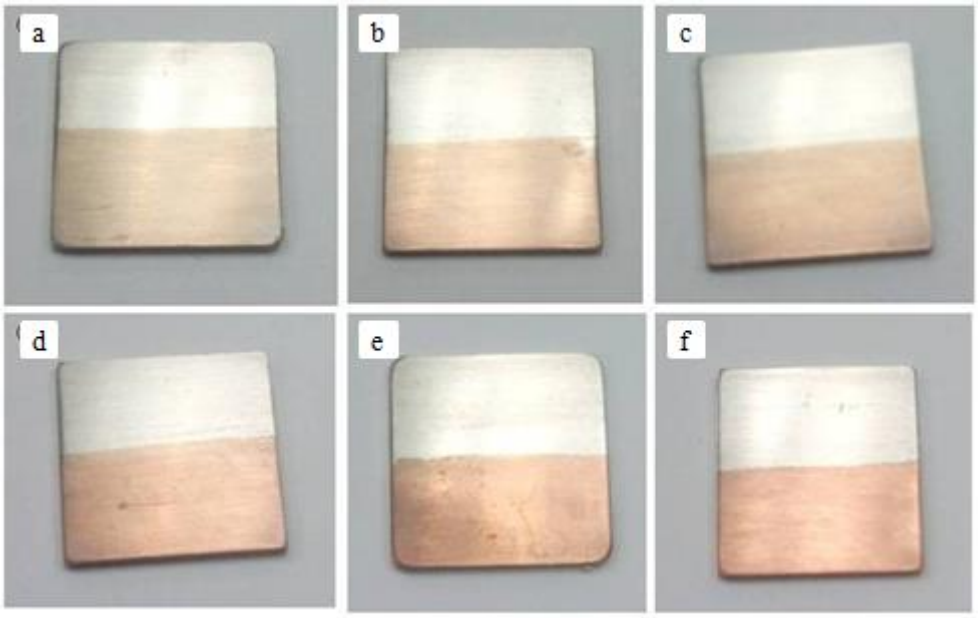

Figure 7. Visual observations of the copper coatings on the stainless steel substrate at -0.25 V for (a) 60 s, (b) 120 s, (c) 180 s, (d) 300 s, (e) 600 s and (f) 900 s. (Note: The substrate can be divided into two layers with top layer is uncoated stainless steel whilst bottom layer indicates copper coated stainless steel)

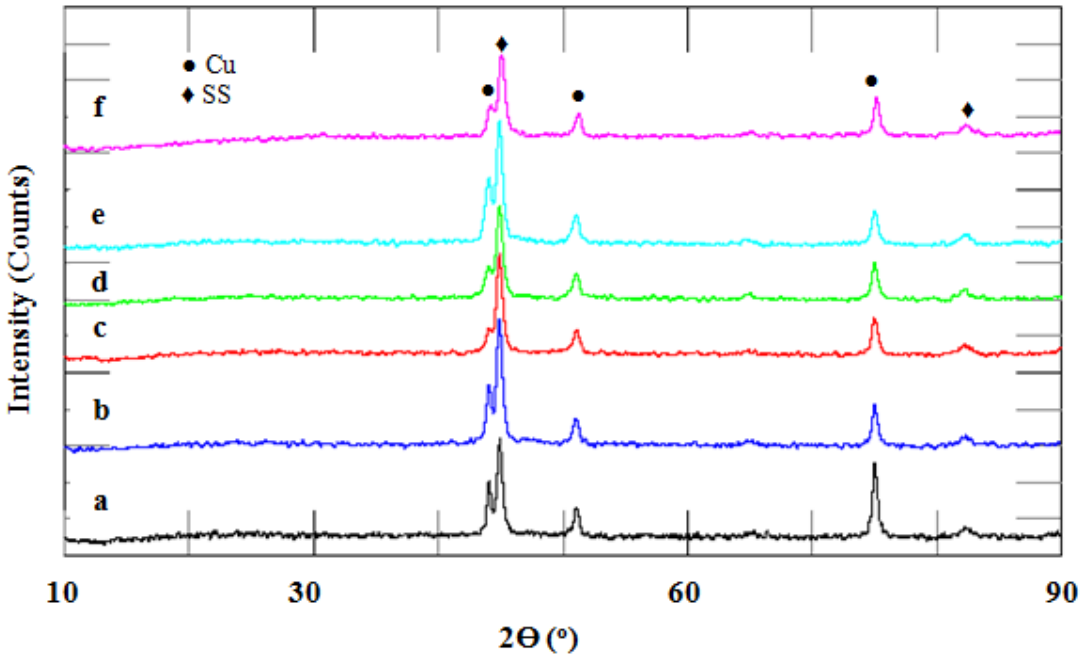

Figure 8. XRD patterns of the copper coatings on the stainless steel substrate at –0.25 V for (a) 60 s, (b) 120 s, (c) 180 s, (d) 300 s, (e) 600 s and (f) 900 s

The XRD patterns of the deposited samples obtained at different deposition times are shown in Fig. 8. Taking no account of the stainless steel peaks, the patterns show that copper coatings

electrodeposited on the stainless steel are crystalline. Three peaks at 2θ values of 43^o, 51^o and 74^o corresponding to (111), (200) and (220) planes of copper are observed and compared with the standard from database reference pattern copper 03-065-9743. The indexed calculations reveal that the copper coatings preferred of face centered cubic (FCC) lattice. For FCC, each h,k,l should be all even or all odd number which can be observed to the (111), (200) and (220) reflections. The peaks related to the copper are a strong agreement with the pattern obtained by Theivasanthi and Alagar [37] for copper nanoparticles and also pattern of copper film electrodeposited on ITO substrate by Ding et al [38].

4. CONCLUSIONS

Copper coating was successfully deposited on stainless steel substrate using pure acidic copper sulphate solution. Prior to electrodeposition, surface pre-treatment was done to remove contamination and oxide layer on stainless steel substrate. Cyclic voltammetry and chronoamperometry methods were applied to study the electrochemical deposition of copper on the stainless steel. Based on chronoamperometric curves, variation of applied potential and deposition time affected the nucleation and growth of the copper coating on stainless steel. Further characterizations of the prepared coatings at different deposition time were done. Surface morphologies by FESEM revealed that spherical particles of copper were deposited on the stainless steel substrate. The density of copper nuclei, particle size and the surface coverage are strongly affected by deposition time. XRD pattern showed copper coatings preferred of faced centered cubic (FCC) lattice.

ACKNOWLEDGEMENTS
The authors wish to acknowledge the Ministry of Higher Education (Malaysia) for the financial support through Fundamental Research Grant Scheme (FRGS) 600-RMI/FRGS 5/3 (139/2015) and Faculty of Applied Sciences, Universiti Teknologi MARA (UiTM) for the facilities provided.

References

1. A. Baral, C.K. Sarangi, B.C. Tripathy, I.N. Bhattacharya and T. Subbaiah, *Hydrometallurgy*, 146 (2014) 8.
2. M. Cloutier, D. Mantovani and F. Rosei, *J. Biotechnol.*, 1295 (2015) 1.
3. H. Palza, K. Delgado and N. Curotto, *Appl. Surf. Sci.*, 357 (2015) 86.
4. A. Augustin, K.R. Udupa, K.U. Bhat and H.A. Chitharanjan, *Mater. Sci. Forum*, 830 (2015) 371.
5. A. Augustin, P. Huilgol, K.R. Udupa and K.U. Bhat, *J. Mech. Behav. Biomed. Mater.*, 63 (2016) 352.
6. A. Augustin, K.R. Udupa and K.U. Bhat, *Perspective in Science*, 8 (2016) 472.
7. A.Y. Nikiforov, X. Deng, I. Onyshchenko, D. Vujosevic, V. Vuksanovic, U. Cvelbar, N.D. Geyter, R. Morent and C. Leys, *Eur. Phys. J. Appl. Phys.*, 75 (2016) 24710.
8. J.W. Dini and D.D. Snyder, *Modern Electroplating*, John Wiley & Sons, Inc., Hoboken, NJ, USA (2010).
9. X. Wang, L.A. Cao, G. Yang and X.P. Qu, *Microelectron. J.*, 164 (2016) 7.

10. T. Chang, Y. Jin, L. Wen, C. Zhang, C. Leygraf, I.O. Wallinder and J. Zhang, *Electrochim. Acta*, 211 (2016) 245.
11. F.C. Walsh and C.T.J. Low, *Surf. Coat. Tech.*, 304 (2016) 246.
12. Y. Yang, Y. Li and M. Pritzker, *Electrochim. Acta*, 213 (2016) 225.
13. P.Y. Chen and Y.T. Chang, *Electrochem. Acta*, 75 (2012) 339.
14. C.V. Pecequilo and Z. Panossian, *Electrochim. Acta*, 55 (2010) 3870.
15. M.A. Pasquale, L.M. Gassa and A.J. Arvia, *Electrochim. Acta*, 53 (2008) 5891.
16. C.S. Lai, X.X. Hu, S. Yau, W.P. Dow and Y.L. Lee, *Electrochim. Acta*, 203 (2016) 272.
17. D. Grujicic and B. Pesic, *Electrochim. Acta*, 47 (2002) 2901.
18. O. Ghodbane, L. Roué and D. Bélanger, *Electrochim. Acta*, 52 (2007) 5843.
19. M.R. Majidi, K. Asadpour-Zeynali and B. Hafezi, *Electrochim. Acta*, 54 (2009) 1119.
20. R.S. Arratia, H.A. Meneses, R.S. Guzman and C.C. Jara, *Lat. Am. Appl. Res.*, 42 (2012) 371.
21. M. Bao, D. Wang, S. Liu, L. Kuang, J. Sun, F. Wang and Y. Wen, *Appl. Surf. Sci.*, 258 (2012) 8008.
22. C.H. Cho, H.S. Shin and C.N. Chu, *Surf. Coat. Tech.*, 222 (2013) 15.
23. S. Joseph and P.V. Kamath, *Solid State Science*, 10 (2008) 1215.
24. M. Rafizadeh, M. Bahmani and R.T. Chelaras, *Port. Electrochim. Acta*, 24 (2006) 387.
25. T.I. Török, V. Orosz, Z. Fekete and G. Szirmai, *Mater. Sci. Eng.*, 37(2) (2012) 99.
26. J.C. Ballesteros, E. Chainet, P. Ozil, Y. Meas and G. Trejo, *Int. J. Electrochem. Sci.*, 6 (2011) 1597.
27. C. Muedre, L. Ricq, J.Y. Hihn, V. Moutarlier, A. Monnin and O. Heintz, Su*rf. Coat. Tech.*, 252 (2014) 93.
28. M. Ojeil, C. Jermann, J. Holah, S.P. Denyer and J.Y. Maillard, *J. Hosp. Infect.*, 85 (2013) 274.
29. P. Airey and J. Verran, *J. Hosp. Infect.*, 67 (2007) 271.
30. M. Ibrahim, F. Wang, M. Lou, G. Xie, B. Li, Z. Bo, G. Zhang, H. Liu and A. Wareth, *J. Biosci. Bioeng.*,112 (2011) 570.
31. J.O. Noyce, H. Michels and C.W. Keevil, *J. Hosp. Infect.*, 63 (2006) 289.
32. P.J. Kuhn, *Diagnostic Medicine* (1983) 62.
33. C. Muedre, L. Ricq, J.Y. Hihn, V. Moutarlier, A. Monnin and O. Heintz, *Surf. Coat. Tech.*, 252 (2014) 93.
34. N. Okamoto, F. Wang and T. Watanabe. *Mater. Trans.*, 45 (2004) 3330.
35. D. Grujicic and B. Pesic, *Electrochim. Acta*, 60 (2005) 4426.
36. A. Mallik and B.C. Ray, *Int. J. Electrochem.*, 2011 (2011) 1.
37. T. Theivasanthi and M. Alagar, *Int. J. Phys. Sci.*, 6 (2013) 662.
38. Y. Ding, J. Zhao, D. Zhang, S. Song and G. Wang, *Surf. Coat. Tech.*, 307 (2016) 177.